Evaluation of AATSR and TMI Satellite SST Data

Richard W. Reynolds
NOAA National Climatic Data Center, Asheville, North Carolina

Chelle L. Gentemann
Remote Sensing Systems, Santa Rosa, CA

Gary K. Corlett
University of Leicester, Leicester, UK

Corresponding author address: Richard W. Reynolds. NOAA's National Climatic Data Center, 151 Patton Avenue, Asheville, NC, 28801-5001
E-mail: Richard.w.reynolds@noaa.gov

Abstract

The purpose of this paper is to investigate two satellite instruments for SST: the infrared (IR) Advanced Along Track Scanning Radiometer (AATSR) and the microwave (MW) Tropical Rainfall Measuring Mission (TRMM) Microwave Imager (TMI). Because of its dual view, AATSR has a potential for lower biases than other IR products such as the Advanced Very High Resolution Radiometer (AVHRR), while the tropical TMI record was available for a longer period of time than the global MW instrument, Advanced Microwave Scanning Radiometer (AMSR).

The results show that the AATSR IR retrievals are good quality with biases lower than or as low as other satellite retrievals between 50°S and 50°N. Furthermore, the dual view algorithm reduces the influence of aerosol contamination. However, the AATSR coverage is roughly half that of AVHRR. North of 50°N there do appear to be biases and high variability in summer daytime retrievals, with smaller but consistent biases observed below 50°S. TMI data can significantly improve coverage off shore in regions where IR retrievals are reduced by cloud cover. However, TMI data have small-scale biases from land contamination that should be removed by modifying the land-sea mask to remove more coastal regions.

1. Introduction and purpose

The Group for High-Resolution Sea Surface Temperature (GHRSST) (see Donlon et al., 2007) has improved and standardized access to a number of different satellite data sets. These improvements have led to a number of global and regional daily SST analyses. Analyses convert irregular spaced data in time and space into regular gridded fields. The purpose of most GHRSST analyses is to obtain the highest accuracy and resolution possible. These two goals often conflict with each other because as resolution increases, the relative number of grid boxes without local data decreases along with accuracy. For example, infrared (IR) satellite retrievals have higher spatial resolution than microwave (MW) retrievals while open ocean MW retrievals have better coverage. If an IR instrument produces a 4 km resolution while a MW instrument produces a 25 km resolution, how will the 4 km resolution be maintained when the 4 km data are missing? Because of the coverage difference, Reynolds et al. (2007) found a large increase in standard deviation and tighter gradients when Advanced Microwave Scanning Radiometer (AMSR) retrievals were added to a daily optimum interpolation (OI) analysis using only Advanced Very High Resolution Radiometer (AVHRR) retrievals. Because of this change in variability Reynolds et al. (2007) has two analyses: AVHRR-only (using AHVRR and in situ data) and AMSR+AVHRR (using AMSR, AVHRR and in situ data).

The purpose of this paper is to look at two additional polar orbiting satellite datasets to determine how adding them would impact the AVHRR-only and AMSR+AVHRR analyses. The two satellite datasets considered are: the Advanced Along Track Scanning Radiometer (AATSR)

and the Tropical Rainfall Measuring Mission (TRMM) Microwave Imager (TMI). AATSR was selected because it has a potential for lower biases compared to AVHRR as will be discussed in the next section. TMI was selected because of the strong impact the global MW instrument, AMSR, has on analyses in mid-latitudes. Two main questions will be considered. What are the biases of these two instruments? What is the impact of using these data in an analysis and are separate analysis versions necessary? To answer these questions, in situ data from ships and buoys and satellite data from AVHRR and AMSR will be used. Analysis procedures make nonlinear processing choices which filter and effectively 'color' the final result. Thus, to access the accuracy of AATSR and TMI data, only one analysis product will be used. A separate paper is being prepared comparing different analysis products.

2. Data

The AATSR is a precision radiometer designed for the accurate retrieval of SST from space for climate applications (Llewellyn-Jones et al., 2001). The SST is retrieved from an algorithm based on radiative transfer theory (see for example Závody et al., 1995, and Merchant et al., 1999), which perform a regression of SST to simulated brightness temperatures with nominal band centers located at 3.7 μm, 11 μm and 12 μm, utilizing either the nadir view or a combination of the nadir and forward views. The 3.7 μm channel has solar contamination during the day. Thus, two different retrievals are implemented, namely dual view 2-channel, mainly

daytime, and dual view 3-channel, only at nighttime. SST fields are provided as either a 1 km swath product, or as a gridded spatially averaged product at several resolutions. Here, single swath 10 arcminute (~ 18 km at the equator) resolution data, referred to as the Meteo product, have been used by first creating daily composite files for daytime and nighttime prior to ingestion into the analysis. A residual retrieval bias (Merchant et al., 2006) is accounted for by the addition of a latitudinal dependent correction to all dual view retrievals according to Birks (2006). An assessment of the accuracy of the Meteo product from AATSR was provided by O'Carroll et al. (2006), who found that the AATSR had a global bias of ~ 0.2 K. As the AATSR bias is of a similar size to the skin minus bulk SST difference (Donlon et al., 2002), no additional adjustment was applied to convert the AATSR skin SST to an equivalent bulk depth.

Accurate microwave SSTs from TMI are available from December 1997 through present. Orbiting at an altitude of about 400 km, this sun-asynchronous satellite is in an equatorial orbit retrieving data within 39 degrees latitude of the equator. The orbit precesses through the diurnal cycle, measuring a complete cycle every 23 days (Kummerow et al., 1998). TMI has 8 channels, corresponding to 4 frequencies (11, 19, 24 and 37 GHz) and two polarizations (vertical and horizontal). This is the first microwave radiometer capable of accurate global SSTs since the poorly calibrated Scanning Multichannel Microwave Radiometer (SMMR) was launched in 1987 (Wentz et al., 2000). (In addition to SST, TMI also measures surface wind speed, atmospheric water vapor, cloud liquid water and rain rate.) Between 4 and 11 GHz the vertically polarized brightness temperature of the sea-surface has an appreciable sensitivity to SST. In addition to

SST, the brightness temperature depends on the sea-surface roughness and on the atmospheric temperature and moisture profile. Fortunately, the spectral and polarimetric signatures of the surface-roughness and the atmosphere are quite distinct from the SST signature, and the influence of these effects can be removed given simultaneous measurements at multiple frequencies and polarizations. All channels are used to simultaneously retrieve SST, wind speed, columnar water vapor, cloud liquid water, and rain rate (Wentz and Meissner, 2000) using a multi-stage linear regression algorithm derived through comprehensive radiative transfer model simulations. SST retrieval is prevented only in regions with sun glint, rain, and near land. Since only a small number of retrievals are unsuccessful, almost complete global coverage between 39°S and 39°N is achieved daily. Any errors in retrieved wind speed, water vapor or cloud liquid water may result in errors in retrieved SST.

3. Data comparisons

Analyses using different in situ and satellite products all need a reference field. Reynolds et al. (2007) uses in situ (ship and buoy) data as the standard. Other analyses may use a satellite product or a climatology. Some adjustment of satellite data is necessary because of small satellite biases which must be corrected to avoid discontinuities between satellite products. Of course these discontinuities can also occur simply due to different diurnal variability measured by the satellites at different observation times

The analysis procedure used here is version 2 of the daily OI which is done on a 1/4° spatial grid. Differences between version 1 (Reynolds et al., 2007) and version 2 are relatively small and mostly consist of additional temporal smoothing[1]. In particular three days of data were used in version 2 where the off days (the day before and after the analysis day) have a reduced weighting (the noise-to-signal standard deviation was doubled) compared to the central day.

In the daily OI all the satellite data are adjusted to both ship and buoy data. As discussed in Reynolds and Smith (1994) ship data have larger random errors than buoy data. These differences can be accounted for in an OI procedure. However, any biases must be corrected before the OI. Furthermore, buoy data were very sparse before about 1989 (e.g., see Reynolds et al., 2002). Thus, ship data need to be used, and ship biases need to be corrected. The method of measuring almost all SST observations from ships has changed over time from temperatures measured from uninsulated and insolated buckets to temperatures measured at engine room intakes. Kent and Taylor (2006) have shown that ship observations made using buckets tend to be biased cold due to evaporation, while ship observations from engine room intake tend to be biased warm due to engine room heating. The location, type, and frequency of measurements continually evolve. To determine the overall bias, monthly averaged ship biases were computed with respect to buoys. However, even with temporal smoothing, differences occurred at irregular intervals and did not seem to be related to seasonal or ENSO events. Monthly scatter plots of the collocated average global ship and buoy anomaly were computed as discussed in the Appendix.

[1] http://www.ncdc.noaa.gov/oa/climate/research/sst/papers/whats-new-v2.pdf

A linear fitting procedure indicated that ships were warmer than buoys by 0.13°C. When the average global difference was computed directly, the ships were found to be warmer than buoys by 0.14°C. As differences of 0.01°C were not significant, 0.14°C was subtracted from all ship data before they were used in the satellite bias correction and in the OI analysis. No adjustments were made to the buoy data.

In the results which follow, important differences among satellite products will be presented. Some of these differences can be attributed to the sampling time and the influence of the diurnal cycle. However, others are more difficult to explain especially at night when the diurnal signal is very weak. Thus, it is critical to choose some standard and correct all data products to it. In the analyses presented here, buoy and bias corrected ship data are used. In many GHRSST products, AATSR data are used as the standard. There is no 'best' answer to this problem. For example using ship and buoy data requires smoothing in space and time because these data are sparse. Thus, some small scale biases will be uncorrected. Furthermore, there are regions, especially at high latitudes, were there are almost no in situ data and hence bias correction is difficult. Using one satellite instrument, e.g., AATSR, as a bias correction standard is also risky because the correction is based on one instrument whose accuracy can deteriorate with time or even fail completely.

The bias correction was performed using empirical orthogonal teleconnections (EOT) functions (see Van den Dool et al. 2000). Smith and Reynolds (2003) used the SST anomalies from Reynolds et al. (2002) analysis to define a set of 130 spatial EOT modes. To determine the

satellite biases, SST anomalies were computed separately for satellite and in situ data anomalies for a 15-day period on a 2° spatial grid. EOT modes were then independently fit to the two anomaly data sets with the restriction that modes were not used unless the data coverage for that mode were adequate for both the in situ and satellite anomaly fields. The restriction and other details of this procedure are described in detail in Reynolds et al. (2007). The difference between the two reconstructed EOT fitted fields was then defined as the satellite bias adjustment. Because the EOT bias correction cannot be carried out without adequate in situ data, a zonal bias correction is made at high southern and northern latitudes were the EOT modes cannot be used. The adjustment was applied separately for day and night for each satellite instrument. The corrected satellite data were then used in the daily OI.

In the comparison to follow, the daily OI AMSR+AVHRR analysis will be used as the standard. It would be better to use the buoy and corrected ship data directly. However, the number of direct comparisons would be greatly reduced because of the scarcity of in situ data and the need to restrict comparisons to collocated space and time data pairs. To better justify the choice of the AMSR+AVHRR analysis instead of the in situ data, the uncorrected ship and buoy data were compared with the daily OI analysis using AMSR+AVHRR data. Here daily ship and buoy observations were averaged onto a 1/4° grid and subtracted from the daily analysis at the same grid point. The daily zonal difference is shown for three bands in Fig. 1. The ship variability is larger than the buoys as expected (Reynolds and Smith, 1994) and the ship variability in the 90°S-20°S band is larger than the ship variability in the other bands because of

the limited ship traffic in the southernmost band. The average uncorrected ship biases for the three bands from south to north are: 0.08, 0.13, and 0.18°C. The average buoy biases south to north are 0.00, 0.02, and 0.02°C. The ship and buoy biases should be 0.14°C and 0°C, respectively. Thus, the AMSR+AVHRR analysis can be expected to be a satisfactory satellite standard for comparison. However, there will be regions with sparse in situ data or regions where biases have small spatial scales. In those cases the AMSR+AVHRR analysis will not be corrected properly as will be discussed in more detail below. However, with these restrictions in mind, 'bias' will be defined as the difference with respect to the AMSR+AVHRR daily OI for the remainder of this paper.

First, it is useful to examine the coverage of different satellite and in situ data. The coverage was computed as a percentage of 1/4° ocean boxes with data compared to the total number of ocean boxes. Here boxes were weighted by the cosine of the latitude, and boxes covered by sea ice are counted as ocean boxes. The average global and tropical daily coverage for 2006-08 is shown in Table 1 for AVHRR (NOAA-17 and 18) AMSR, AATSR, TMI, ships and buoys. The global AVHRR had typical daytime coverage near 10%, with nighttime coverage 2-3% higher. Global daytime AATSR coverage was just above 5% for day and nighttime. The AATSR coverage (see Table 1) is roughly half that of AVHRR because the AATSR swath width is narrower. The Global AMSR coverage was between 40% for daytime, with nighttime coverage 10% higher. (AVHRR and AMSR daytime coverage is lower relative to night due to sun glint. In addition, the AVHRR daytime coverage is further reduced by defining

solar angles less than 75° as day, A. Ignatov, personal communication, 2009.) The TMI coverage was nearly 30%, lower than AMSR because TMI data were only used between 35°S-35°N. The tropical coverage shows that the AMSR and TMI coverage was very similar. Satellite data all have at least 10 times the coverage of either ships or buoys.

To examine global satellite biases, daytime and nighttime differences were computed with respect to the AMSR+AVHRR daily OI. These differences will henceforth be referred to as biases. The average daytime biases for 2006-08 are shown in Fig. 2. NOAA-17 and AATSR have morning equatorial crossings while NOAA-18 and AMSR have afternoon equatorial crossings. Thus, the diurnal cycle should impact both NOAA-18 and AMSR as shown by the warmer biases in the figure between roughly 60°S and 60°N. However, the NOAA-18 biases in this region were larger than the AMSR values. Also the AMSR biases tended to be more positive than the NOAA-17 biases. Outside of this range and in the Davis Strait (between Greenland and Canada), in situ observations were low and it is difficult to know which differences are actually biases. AATSR had the largest positive biases at latitudes north of 70°N and negative biases south of 60°S. However, in situ data were sparse in these regions so the analysis accuracy is uncertain.

The standard deviation of the daytime biases is shown in Fig. 3 for June-August 2006-08. AATSR showed larger values than any of the other products north of 35°N. This may be due to AATSR's reduced sampling compared to the others. For other seasons for day and for all seasons for night, the AATSR standard deviation was not especially larger than the other products.

The average nighttime biases for 2006-08 are shown in Fig. 4. The nighttime biases are especially important because there is no diurnal warming signal within them. As expected, nighttime biases are smaller than the daytime biases. The buoy and corrected in situ data used in the AMSR+AVHRR daily OI are based on 15-days of data. This strongly suppressed any diurnal cycle in the daily OI. The consistent negative biases in the eastern equatorial Pacific for all nighttime satellite products suggest that the bias corrections in the daily OI may not be correct there. In addition, it is not clear why both AVHRR biases near 60°S were positive and why they were larger for NOAA-18. AATSR had the largest negative biases at latitudes north of 70°N and south of 60°S. To examine these biases in more detail, the nighttime zonal averages are shown in Fig. 5. The zonal biases were only shown between 60°S and 60°N to help ensure that there was sufficient in situ data to define the biases. However, even if the reference OI is not perfect, this figure makes it clear that average zonal differences among satellite products were typically 0.1°C and may exceed that value south of 50°S and north of 50°N.

It is more difficult to separate the TMI biases into day and night because the TRMM satellite is not sun synchronous and because the TMI retrievals are restricted to the tropics. Thus, biases are shown for a smaller region in the Tropical Atlantic in Fig. 6 where TMI

ascending and descending orbits were added to the nighttime fields shown in Fig. 4. Months of June, July and August are shown because that is period when IR retrievals may be biased cold due to large troposphere aerosols from dust blown off the Sahara Desert (see May et al., 1992 and Vázquez-Cuervo, et al., 2004) The nighttime negative biases for both NOAA-17 and NOAA-18 were very similar although NOAA-18 biases were more negative. Differences between TMI descending and ascending were very close as expected since both descending and ascending parts of the orbit equally sample the diurnal cycle. Aerosols do not impact MW retrievals and the AATSR dual view can compensate for them, although the current retrieval appears to overcorrect resulting in small positive biases in regions of high tropospheric aerosol. Therefore, negative biases should only be expected in AVHRR, which are clearly demonstrated in the figure. The AMSR and TMI biases were even smaller than the IR products. Some of the warm biases off the coast of Africa in TMI may be due to diurnal warming which is included in the TMI data. However, there is clearly land contamination in the TMI retrievals. The relative small scales of the biases cannot be eliminated by the large-scale daily OI bias correction procedure. This can be clearly seen in Fig. 7 which uses the **bias corrected** data. Here all biases are reduced from those in Fig. 6 except for the TMI coastal biases. In future analyses, an extended land-sea mask, available in the GHRSST TMI data as a quality flag, must be used to eliminate the coastal TMI values before they are used in the analysis.

4. Special daily OI analyses

To determine how the data impacted the analysis, several additional daily OI version 2 analyses were computed: AMSR-only, AATSR-only, and TMI+AVHRR. TMI was not analyzed separately because TMI was only used from 35°S to 35°N. These analyses were compared with the operational version 2 AVHRR-only and AMSR+AVHRR analyses. All satellite data were bias corrected using in situ data before being used in any of the OI analyses.

Although AATSR reduced biases in uncorrected areas it should be used with other products in a daily analysis. This can be clearly shown in Fig. 8. In winter cold coastal water lies off the Carolina Coast between the Gulf Stream and the coast. The figure shows that the cold water is not properly resolved in the AATSR-only analysis. The AATSR-only analysis has trouble resolving the colder water because of differential cloud screening that flags clear-sky cold water as being cloudy (see for example Merchant et al., 2005). It is also not resolved in the AMSR-only analysis because MW retrievals cannot be made near land. In addition, the warm water local maximum temperatures along the axis of the flow of the Gulf Stream appear smoother in the daily OI analyses using AMSR, a little rougher in the AVHRR-only analysis, and roughest in the AATSR-only analysis. In the AATSR-only analysis a large bull's-eye occurs at roughly 38°N and 63°W. This strengthened in the AATSR-only analysis with time and persisted until the first week in February. It also appeared in the AVHRR-only analysis although it was a little weaker and disappeared a few days earlier. The bull's-eye was due to bad moored buoy data. The bad data impacted the analyses using IR data because these data were sparse in this region due to winter cloud cover. Because MW data are not impacted by cloud cover, the

AMSR-only and AMSR+AVHRR analyses were able to compensate for the bad buoy data. (TMI was not able to impact the results at 38°N because TMI data were not used north of 35°N.)

In the tropics, TMI had both a positive and negative impact. Figure 9 shows the negative impact for 28 February 2007. Here, the AVHRR-only, AATSR-only and AMSR-only analyses were very similar. However, the TMI+AVHRR analysis showed higher temperatures near the land. This was especially evident near the Solomon Islands (which lie east of New Guinea between 145°E and 160°E). The TMI bias was due to land contamination also illustrated in Figs. 6 and 7. As mentioned earlier the scale of the land contamination was too small to be corrected by the satellite bias correction procedure. Although lower biases did occur on other days, the example shown in Figs 6 and 7 was not unique. A land-sea mask which excluded more coastal regions would eliminate the land contamination from the TMI data.

It is easier to document the positive benefits of AMSR than TMI data, because AMSR retrievals are available in the strong gradients of western boundary currents where winter cloud cover can severely limit IR retrievals. However, a clear example of the benefit of TMI can be seen in equatorial eastern Pacific just west of the Galapagos Islands as shown in Fig. 10. Here the frontal boundary just north of the equator was noisy in the AVHRR-only analysis. In particular, note the front between 100°W and 95°W. The noise occurred because IR retrievals are reduced by cloud cover while the MW retrievals are only reduced by precipitation. Thus, the frontal feature looks more coherent in the AMSR, AMSR+AVHRR and TMI+AVHRR analyses.

5. Conclusion and recommendations

The results show that the AATSR IR retrievals are a high quality product. Overall AATSR biases with respect to in situ data are lower than or as a low as the AVHRR (NOAA-17 and NOAA-18) and AMSR satellite retrievals between 50°S and 50°N. Furthermore, the dual coverage algorithm reduces the influence of aerosol contamination. North of 50°N there do appear to be positive daytime and negative nighttime biases at very high latitudes, as well as high variability in summer daytime retrievals. South of 50°S there are consistent negative biases and both daytime and nighttime retrievals. However, as was noted earlier, the AATSR biases in high latitude regions are difficult to verify using independent in situ data due to the sparseness of in situ data in these regions. In addition, as the AATSR swath is narrower than that of AVHRR, it is recommended that AATSR be used with other satellite data in analyses. The results show that using the present AATSR product as a bias standard may lead to analysis biases, and so it is always necessary to continue to monitor AATSR biases with buoy data to ensure that instrument accuracy does not deteriorate. Also, it is important to point out that buoy data have an advantage of being made by independent instruments. Thus, the bad buoy that was shown in Fig. 8 would not be able to bias the entire analysis. However, buoy data are much sparser than AATSR retrievals, and there are some regions without adequate in situ sampling, and so a combination of AATSR and in situ data may provide the best reference source for the analysis

TMI data were shown to have advantages and disadvantages. TMI data have small scales biases from land contamination. These data can easily be removed by a modifying the land-sea

mask to remove more coastal regions. However, TMI can significantly improve open-ocean coverage in regions where IR retrievals are reduced by cloud cover. AMSR microwave data have a strong impact on analyses in mid-latitudes particularly in high gradient regions such as the Gulf Stream. TMI doesn't have this impact because accurate TMI retrievals are limited to the tropics. Thus, when TMI was added to AVHRR there was no large variability increase as there was when AMSR was added to AVHRR. Therefore, it is not essential that a separate version of the daily OI analysis be maintained with and without TMI data.

Acknowledgments. We are grateful to NCDC and the NOAA Office of Global Programs, which provided partial support for this work. The graphics were computed using the Grid Analysis and Display System (GrADS) (http://grads.iges.org/grads), Center for Ocean-Land-Atmosphere Studies. We also thank Tom Smith, Ken Knapp and Huai-Min Zhang and 2 anonymous reviewers for their constructive advice. Operational SST data from AATSR is provided by the European Space Agency (ESA), http://www.envisat.esa.int. G Corlett is funded by the UK Department of Energy and Climate Change (DECC) through Space ConneXions contract 2004-03-001/CPEG10. C. Gentemann's work was funded by NASA Physical Oceanography, grant NNH08CC60C.

APPENDIX

Ship SST Biases with Respect to Buoys

As discussed in Reynolds and Smith (1994) and Reynolds et al. (2002), the random and bias errors of ship SST data are larger than the random and bias errors of buoy SSTs, and the coverage of buoys tends to increase with time while the coverage of ships tends to decrease. To determine the variability of a globally averaged bias, monthly averaged ship biases were computed with respect to buoys. However, even with temporal smoothing, differences occurred at irregular intervals and did not seem to be related to seasonal or ENSO events.

For January 1989 - December 2006, monthly ship and buoy observations were averaged onto a 2° grid and converted to anomalies relative to the Xue et al. (2003) 1971-2000 climatology. For each month, globally averaged anomalies were computed over 2° grid boxes which had both ship and buoy data. Scatter plots of the average global ship and buoy monthly anomaly SSTs are shown in Fig. A-1 for two 9-year periods. The least squares linear fit for the two periods is also shown with the slope and intercept and given in Table A-1. The fit indicates that the average intercept is -0.13°C. These results strongly suggest that a spatial and temporal constant bias correction is needed for ship SSTs. Furthermore, finer space and time corrections do not seem to be possible with the limited in situ data available.

References

Birks, A., 2006: Latitude Dependent Bias Correction, AATSR Technical Note, Rutherford Appleton Laboratory (Available from http://earth.esa.int/pcs/envisat/aatsr/articles/).

Donlon, C. and others, 2007: The global ocean data assimilation experiment high-resolution sea surface temperature pilot. *Bull. Amer. Meteor. Soc.*, **88**, 1197-1213.

Donlon, C.J., P.J. Minnett, C. Gentemann, T. J. Nightingale, I. J. Barton, B. Ward, and M. J. Murray, 2002: Toward improved validation of satellite sea surface skin temperature measurements for climate research. *J. Climate*, **15**, 353–369.

Kent, E.C., and P.K. Taylor, 2006: Toward Estimating Climatic Trends in SST. Part I: Methods of Measurement. *J. Atmos. Oceanic Technol.*, **23**, 464–475.

Kummerow, C. D. ,W. Barnes, T. Kozu, J. Shieu, and J. J. Simpson, 1998: The tropical rainfall measuring mission (TRMM) sensor package. *J. Atmos. Oceanic Technol.*, **15**, 809-817.

Llewellyn-Jones, D., M. C. Edwards, C. T. Mutlow, A. R. Birks, I. J. Barton and H. Tait, 2001. AATSR: global-change and surface-temperature measurements from Envisat. *ESA Bulletin*, **105**, 10-21 (http://www.esa.int/esapub/bulletin/bullet105/bul105_1.pdf).

May, D. A., L. Stowe, J. Hawkins, E. P. McClain, 1992: A Correction for Saharan Dust Effects on Satellite Sea Surface Temperature Measurements. *J. Geophys. Res.*, **97**, 3611–3619.

Merchant, C. J., A. R. Harris, M. J. Murray and A. M. Závody, 1999: Toward the elimination of bias in satellite retrieval of sea surface temperature 1. Theory, modeling and inter-algorithm comparison. *J. Geophys. Res.*, **104**, 23565-23578.

Merchant, C. J., A. R. Harris, E. Maturi and S. MacCallum, 2005: Probabilistic physically based cloud screening of satellite infrared imagery for operational sea surface temperature retrieval. *Quart. J. Royal Met. Soc.*, **131**, 2735-2755.

Merchant, C. J., L. A. Horrocks, J. Eyre and A. G. O'Carroll, 2006: Retrievals of sea surface temperature from infra-red imagery: origin and form of systematic errors. *Quart. J. Royal Met. Soc.*, **132**, 1205-1223.

O'Carroll, A. G., J. G. Watts, L. A. Horrocks, R. W. Saunders and N. A. Rayner, 2006: Validation of the AATSR meteo product sea-surface temperature. *J. Atmos. Oceanic Technol.*, **23**, 711–726.

Reynolds, R. W. and T. M. Smith, 1994: Improved global sea surface temperature analyses using optimum interpolation. *J. Climate*, **7**, 929-948.

Reynolds, R. W., N. A. Rayner, T. M. Smith, D. C. Stokes and W. Wang, 2002: An improved in situ and satellite SST analysis for climate. *J. Climate*, **15**, 1609-1625.

Reynolds, R. W., T. M. Smith, C. Liu, D. B. Chelton, K. S. Casey, and M. G. Schlax, 2007: Daily high-resolution blended analyses for sea surface temperature. *J. Climate,* **20***,* 5473-5496.

Smith, T.M., and R.W. Reynolds, 2003: Extended reconstruction of global sea surface temperatures based on COADS Data (1854 1997). *J. Climate*, **16**, 1495-1510.

Van den Dool, H. M., S. Saha, and Å. Johansson, 2000: Empirical orthogonal teleconnections. *J. Climate*, **13**, 1421–1435.

Wentz, F. J., C. L. Gentemann, D. K. Smith, and D. B. Chelton, 2000: Satellite measurements of sea surface temperature through cloud. *Science*, **288**, 847-850.

Wentz, F. J. and T. Meissner, 2000: AMSR Ocean Algorithm, Version 2. RSS Tech. Report 121599A, 66 pp. [Available from Remote Sensing Systems, 438 First Street, Suite 200, Santa Rosa, CA 95401, USA.]

Vázquez-Cuervo, J., E.M. Armstrong, and A. Harris, 2004: The Effect of Aerosols and Clouds on the Retrieval of Infrared Sea Surface Temperatures. *J. Climate*, **17**, 3921–3933.

Xue, Y., T. M. Smith, and R. W. Reynolds, 2003: Interdecadal changes of 30-yr SST normals during 1871-2000. *J. Climate*, **16**, 1601-1612.

Závody, A. M., C. T. Mutlow, and D. T. Llewellyn-Jones, 1995: A radiative transfer model for sea surface temperature retrieval for the along-track scanning radiometer. *J. Geophys. Res.*, **100**, 937–952.

List of Figures

FIG 1. Spatial average daily bias of buoy and uncorrected ship data for three zonal bands: 20°N-90°N (top), 20°S-20°N (middle) and 90°S-20°S (bottom). Biases are defined as differences with respect to the daily OI using AMSR and AVHRR data.

FIG 2. Average (1 January 2006 - 31 December 2008) daytime satellite bias with respect to the daily OI using AMSR and AVHRR data. The top left, top right, bottom left and bottom right panels show the AVHRR NOAA-17, AVHRR NOAA-18, AATSR and AMSR, respectively. The left (right) panels show satellite observations with morning (afternoon) equatorial crossing times.

FIG 3. Daily daytime satellite bias standard deviation bias with respect to the daily OI using AMSR and AVHRR data for June, July and August for 2006 - 2008. Otherwise as in Fig. 2.

FIG 4. Average (1 January 2006 - 31 December 2008) nighttime satellite bias with respect to the daily OI using AMSR and AVHRR data. Otherwise as in Fig. 2.

FIG 5. Zonal and temporal averaged (1 January 2006 - 31 December 2008) nighttime satellite bias with respect to the daily OI using AMSR and AVHRR data.

FIG 6. Average daily satellite bias with respect to the OI for June, July and August for 2006-2008. The top left, top right, middle left, middle right bottom left and bottom right panels show the AVHRR NOAA-17, AVHRR NOAA-18, AATSR, AMSR, ascending TMI, and descending TMI data, respectively.

FIG 7. Average corrected daily satellite bias with respect to the OI for June, July and August for

2006-2008. Otherwise as in Fig 6.

FIG 8. Four daily SST analyses for 14 January 2007. The top left, top right, bottom left and bottom right panels show the daily OI using AVHRR-only, AATSR-only, AMSR-only, and AMSR+AVHRR, respectively.

FIG 9. Four daily SST analyses for 28 February 2008. The top left, top right, bottom left and bottom right panels show the daily OI using AVHRR-only, AATSR-only, AMSR-only, and TMI+AVHRR, respectively.

FIG 10. Four daily SST analyses for 28 January 2007. The top left, top right, bottom left and bottom right panels show the daily OI using AVHRR-only, AMSR+AVHRR, AMSR-only, and TMI+AVHRR respectively.

FIG A-1. Scatter plot of global collocated average monthly ship vs. buoy anomaly for January 1989 - December 2006. The first 9-years are shown in the black and the second 9-years in red. Least squares linear fits for the two periods are also shown.

TABLE 1. Average percentage of global ocean 1/4° boxes with daily data to total ocean boxes. The boxes are weighted by the cosine of latitude; boxes covered with sea ice are counted as ocean boxes.

Type of Data	**Coverage: 90°S-90°N**	**Coverage: 20°S-20°N**
Buoy	0.5%	0.4%
Ship	0.3%	0.2%
Day AVHRR: NOAA-17	9.9%	11.2%
Night AVHRR: NOAA-17	12.9%	16.9%
Day AVHRR: NOAA-18	9.0%	8.9%
Night AVHRR: NOAA-18	11.6%	13.8%
Day AATSR	5.1%	6.4%
Night AATSR	5.3%	7.0%
Day AMSR	43.0%	40.2%
Night AMSR	48.9%	41.5%
Ascending TMI	30.4%	39.1%
Descending TMI	29.7%	39.1%

TABLE A-1. The linear least squares fit of the ship and buoy data shown in Figure A-1.

Period	Slope	Intercept
1989 - 1997	0.99	-0.14°C
1998 - 2006	0.92	-0.12°C
1989 - 2006	0.97	-0.13°C

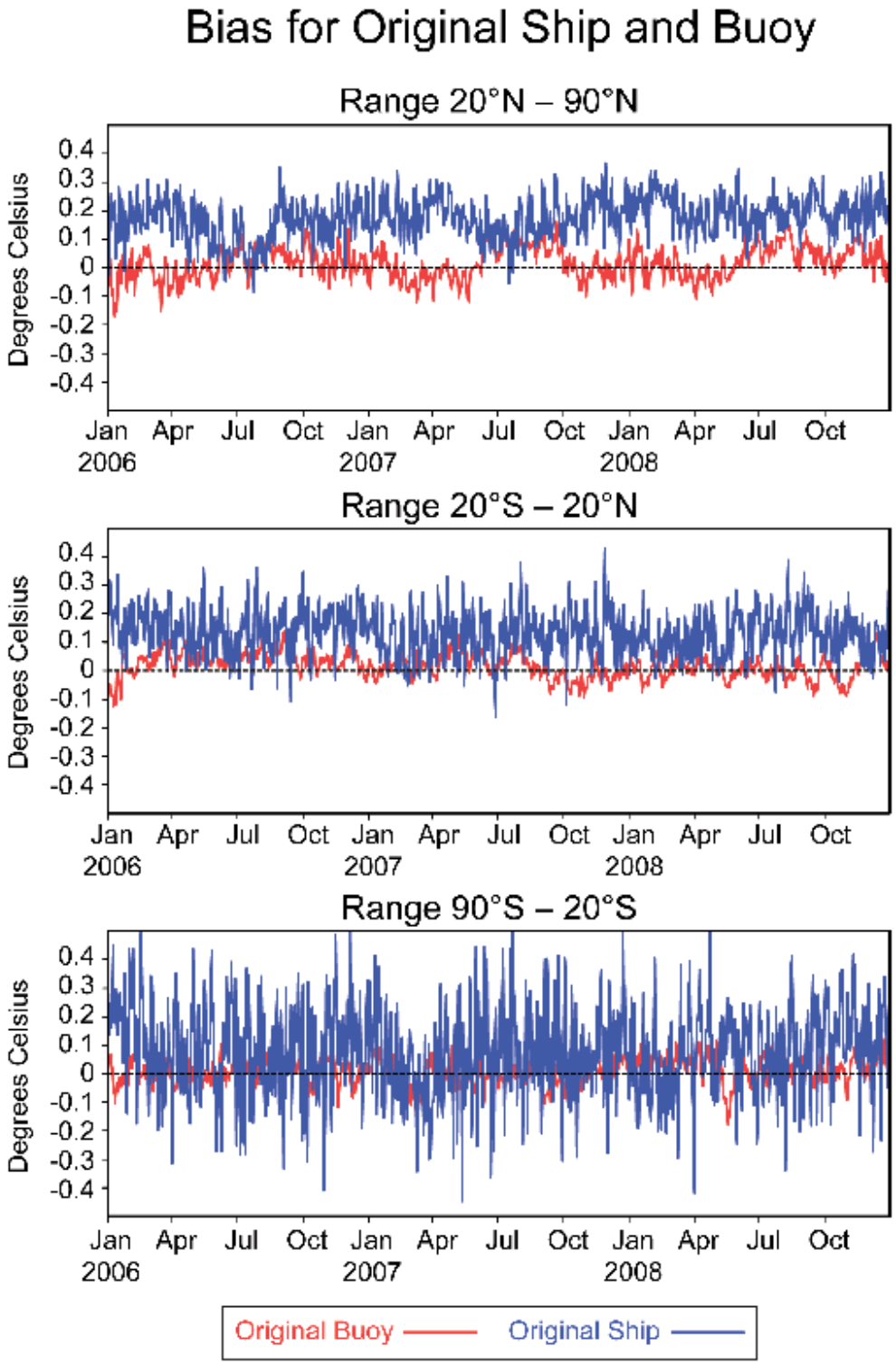

Figure 1. Spatial average daily bias of buoy and uncorrected ship data for three zonal bands: 20°N-90°N (top), 20°S-20°N (middle) and 90°S-20°S (bottom). Biases are defined as differences with respect to the daily OI using AMSR and AVHRR data.

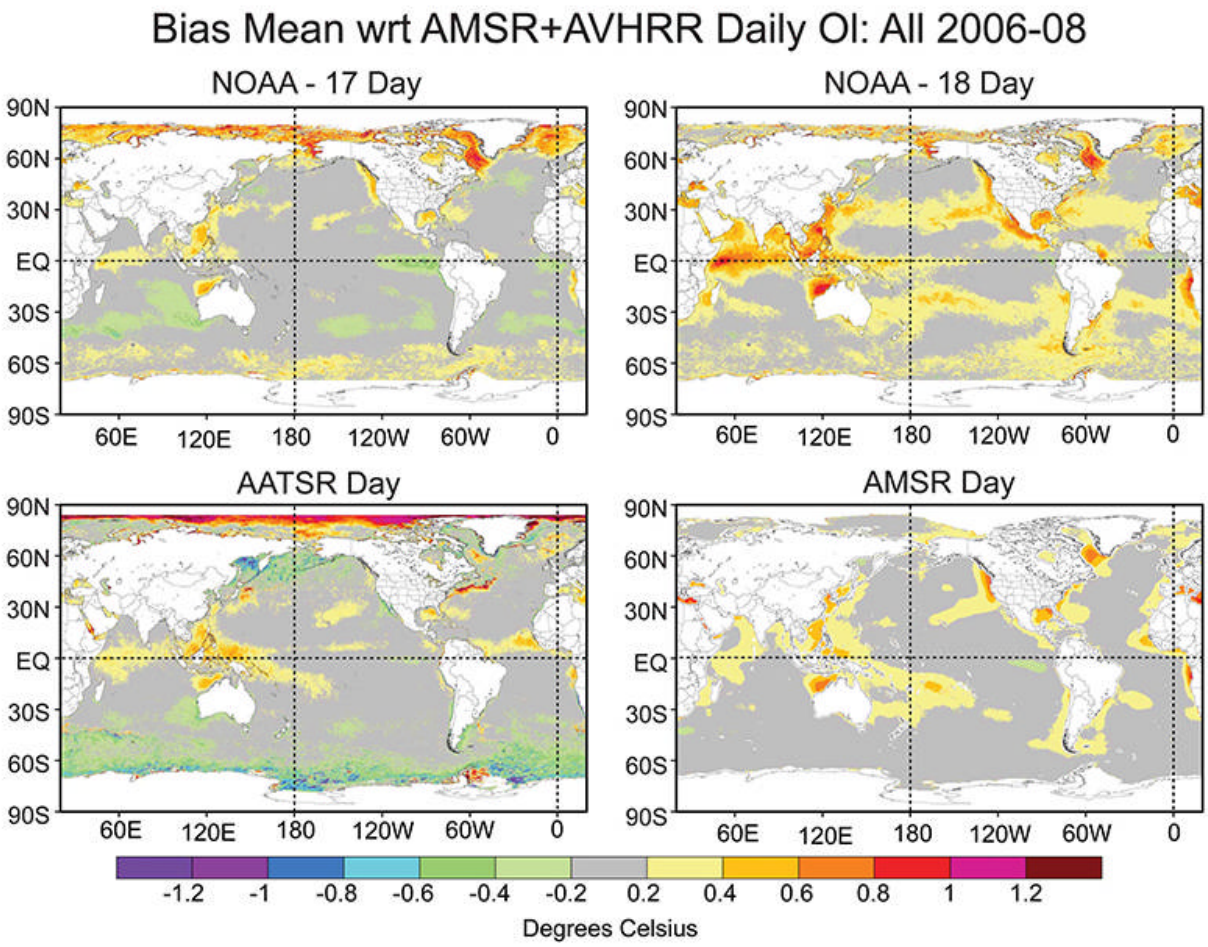

Figure 2. Average (1 January 2006 - 31 December 2008) daytime satellite bias with respect to the daily OI using AMSR and AVHRR data. Average (1 January 2006 - 31 December 2008) daytime satellite bias with respect to the daily OI using AMSR and AVHRR data. The top left, top right, bottom left and bottom right panels show the AVHRR NOAA-17, AVHRR NOAA-18, AATSR and AMSR, respectively. The left (right) panels show satellite observations with morning (afternoon) equatorial crossing times.

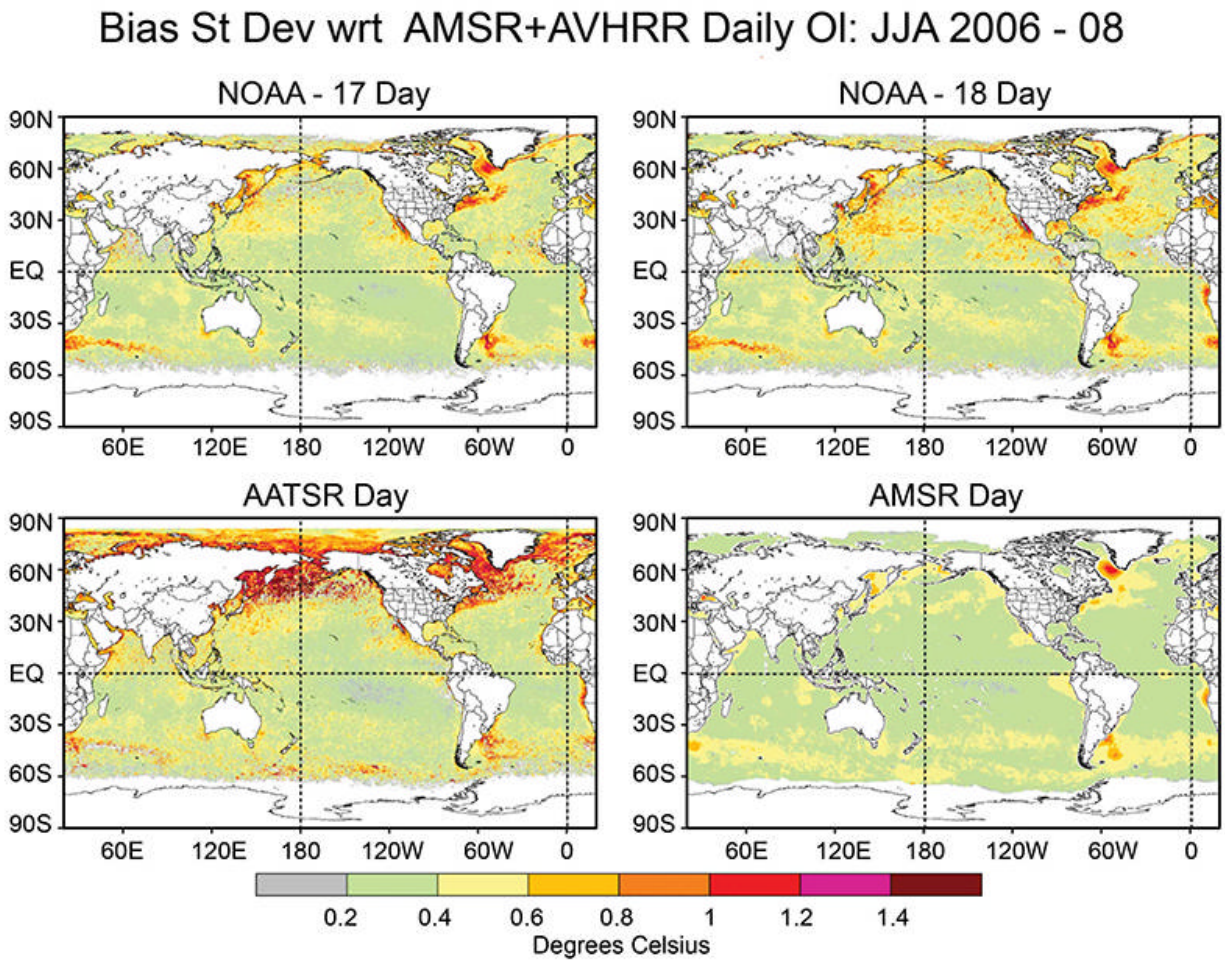

Figure 3. Daily daytime satellite bias standard deviation bias with respect to the daily OI using AMSR and AVHRR data for June, July and August for 2006 - 2008. Otherwise as in Fig. 2.

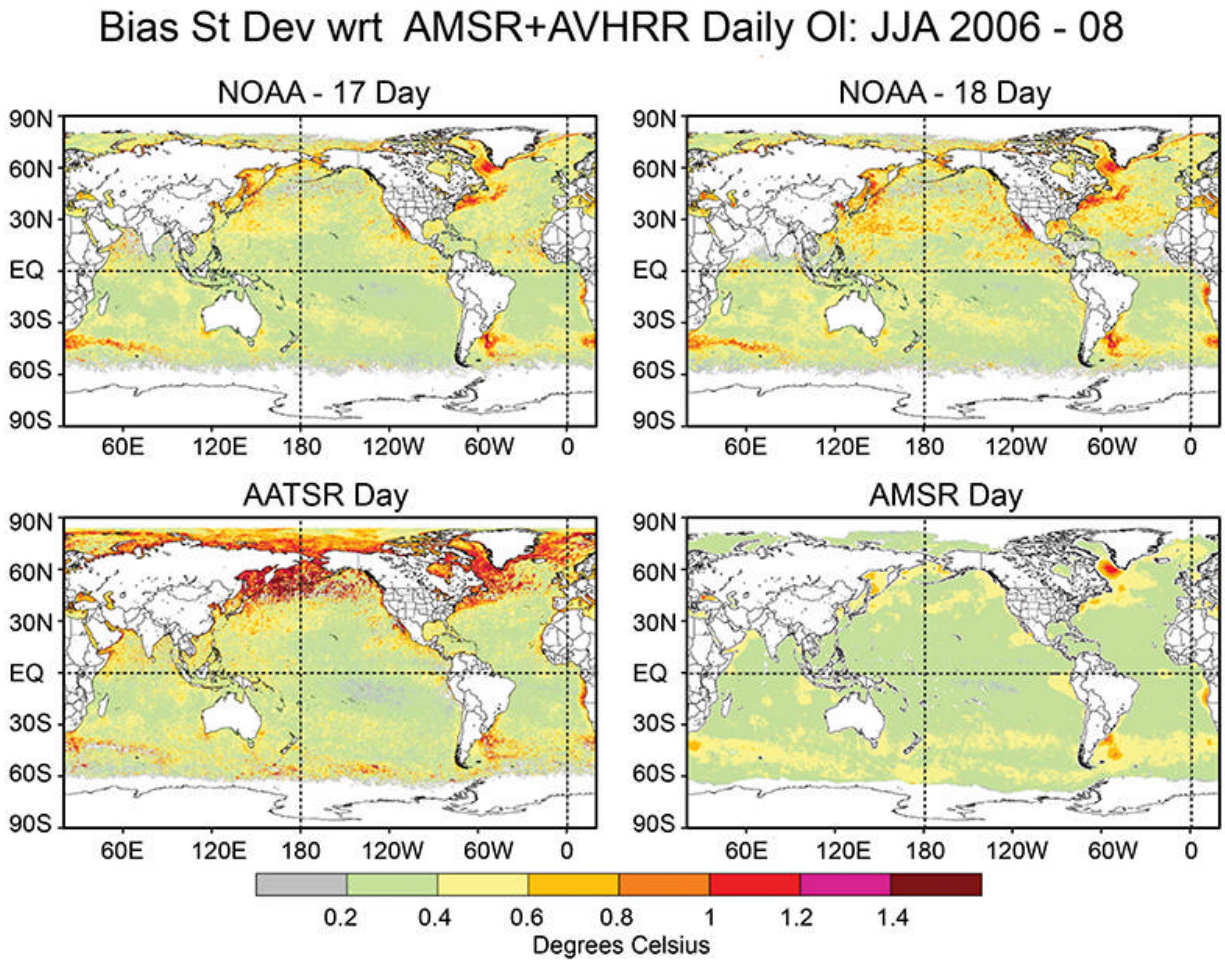

Figure 4. Average (1 January 2006 - 31 December 2008) nighttime satellite bias with respect to the daily OI using AMSR and AVHRR data. Otherwise as in Fig. 2.

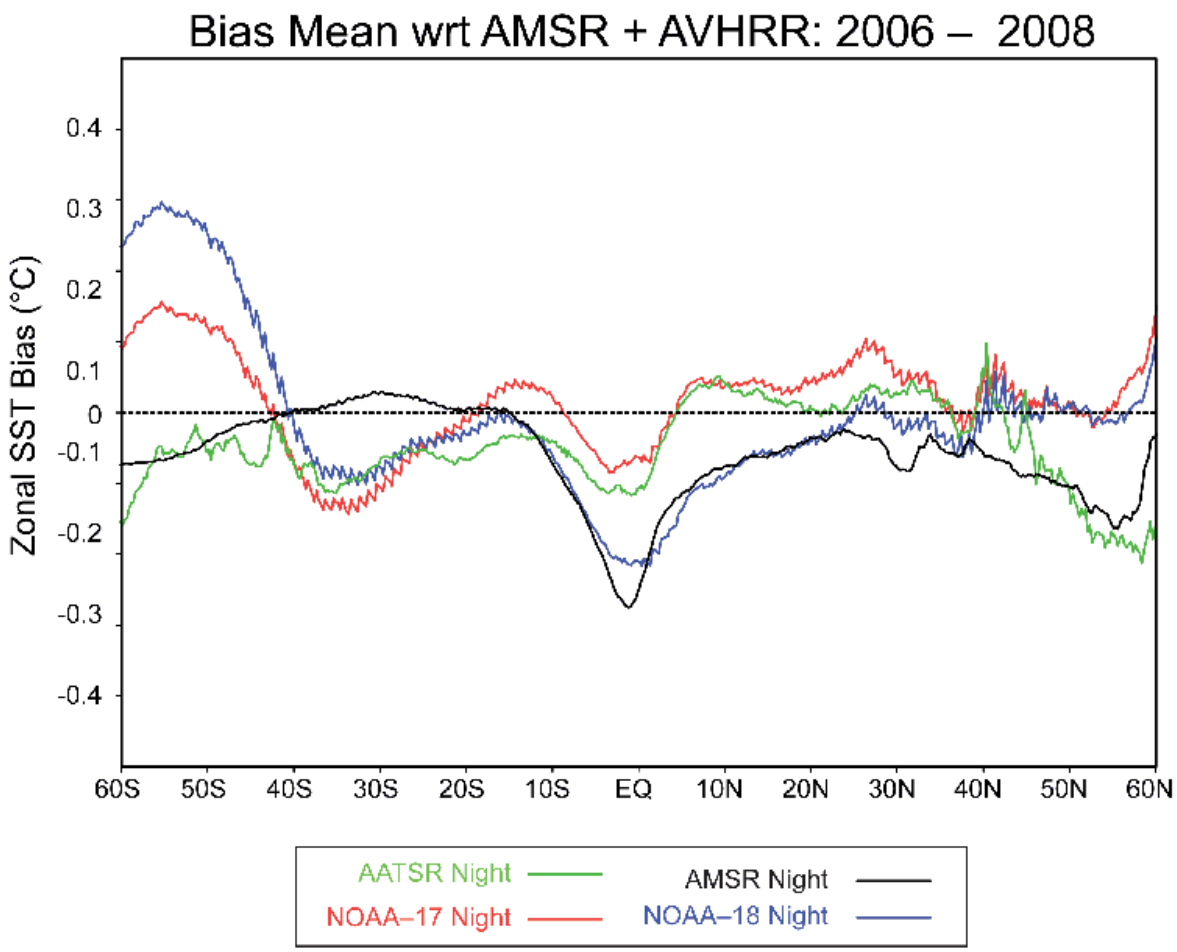

Figure 5. Zonal and temporal averaged (1 January 2006 - 31 December 2008) nighttime satellite bias with respect to the daily OI using AMSR and AVHRR data.

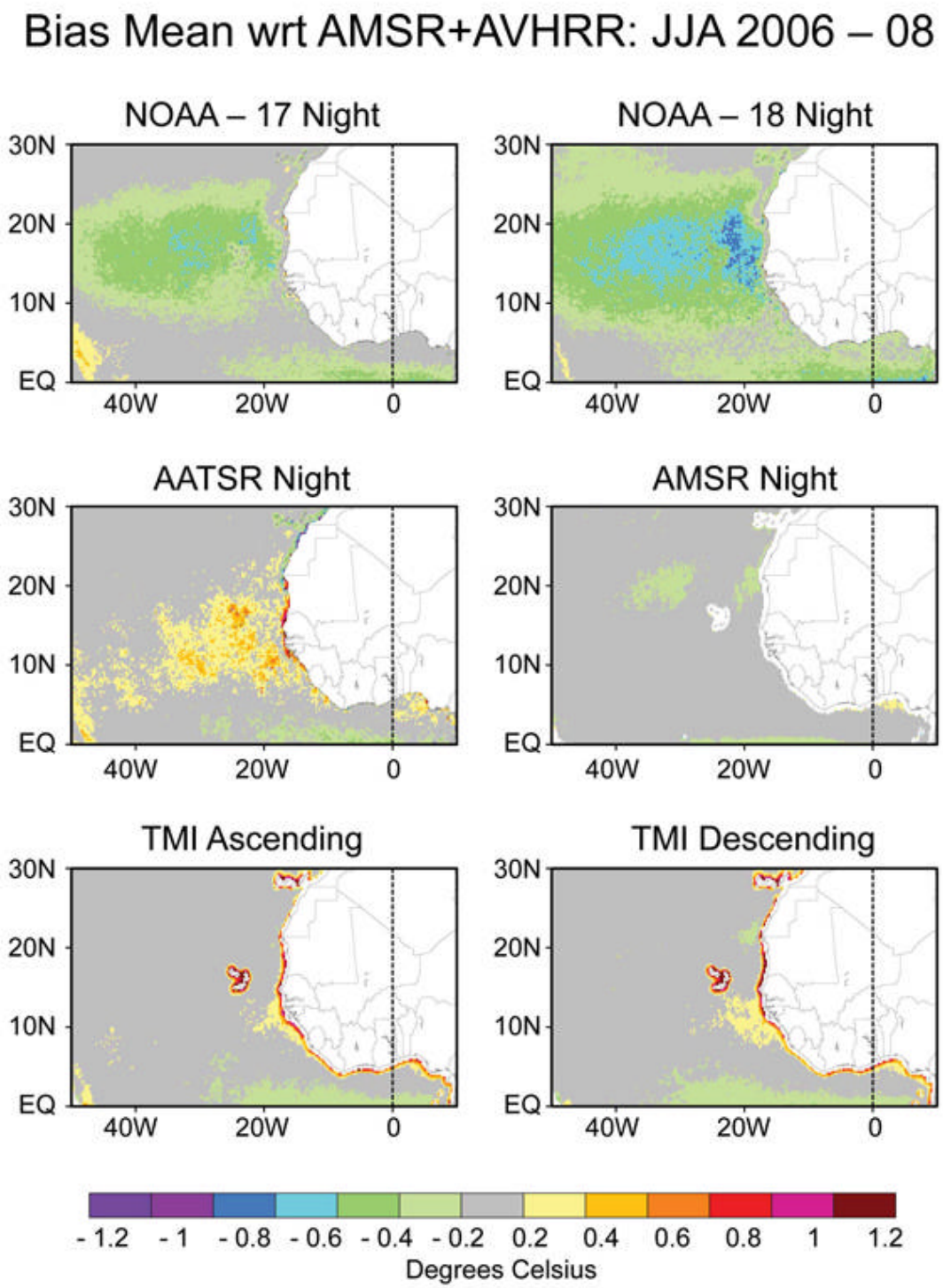

Figure 6. Average daily satellite bias with respect to the OI for June, July and August for 2006-2008. The top left, top right, middle left, middle right bottom left and bottom right panels show the AVHRR NOAA-17, AVHRR NOAA-18, AATSR, AMSR, ascending TMI, and descending TMI data, respectively.

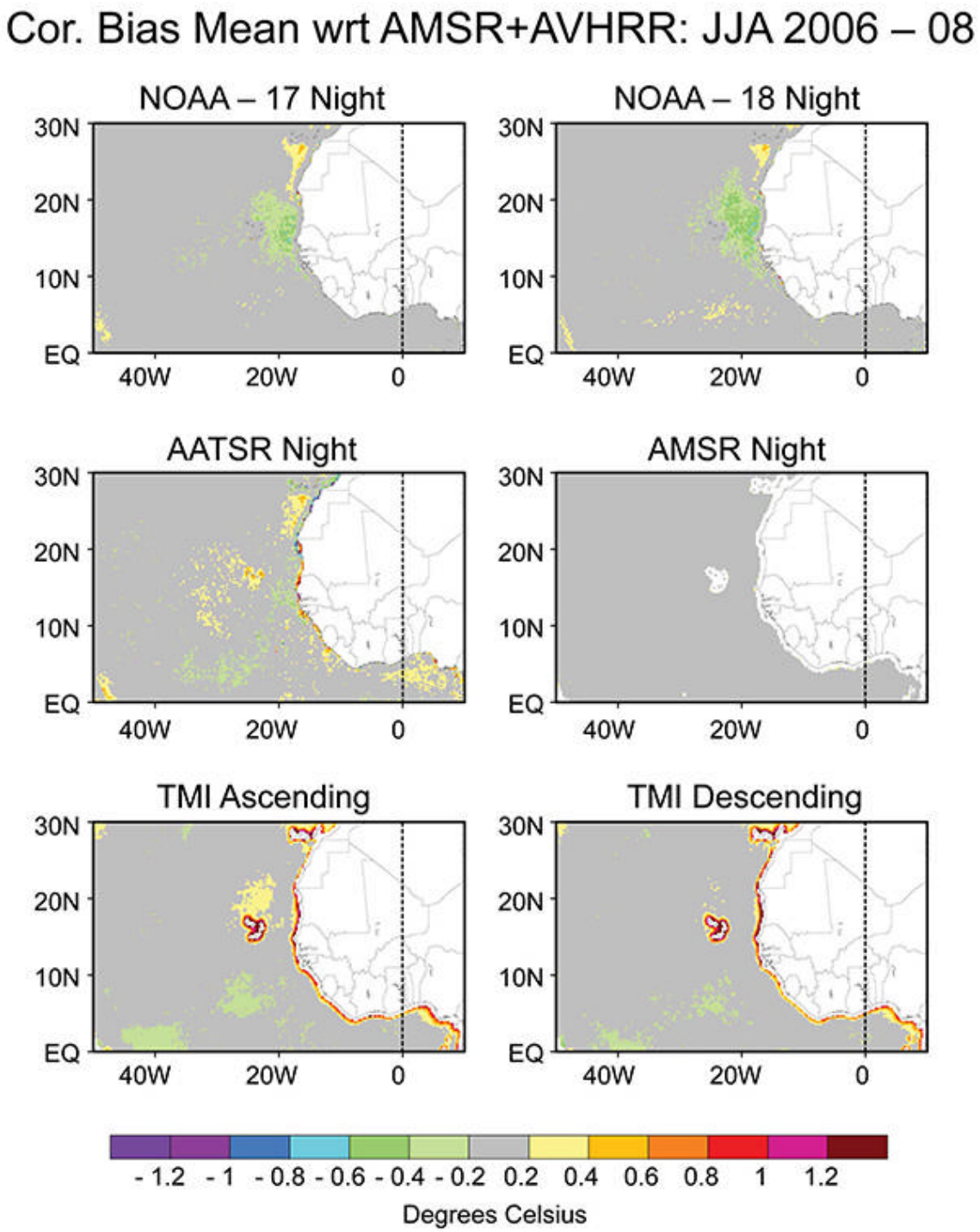

Figure 7. Average corrected daily satellite bias with respect to the OI for June, July and August for 2006-2008. Otherwise as in Fig 6.

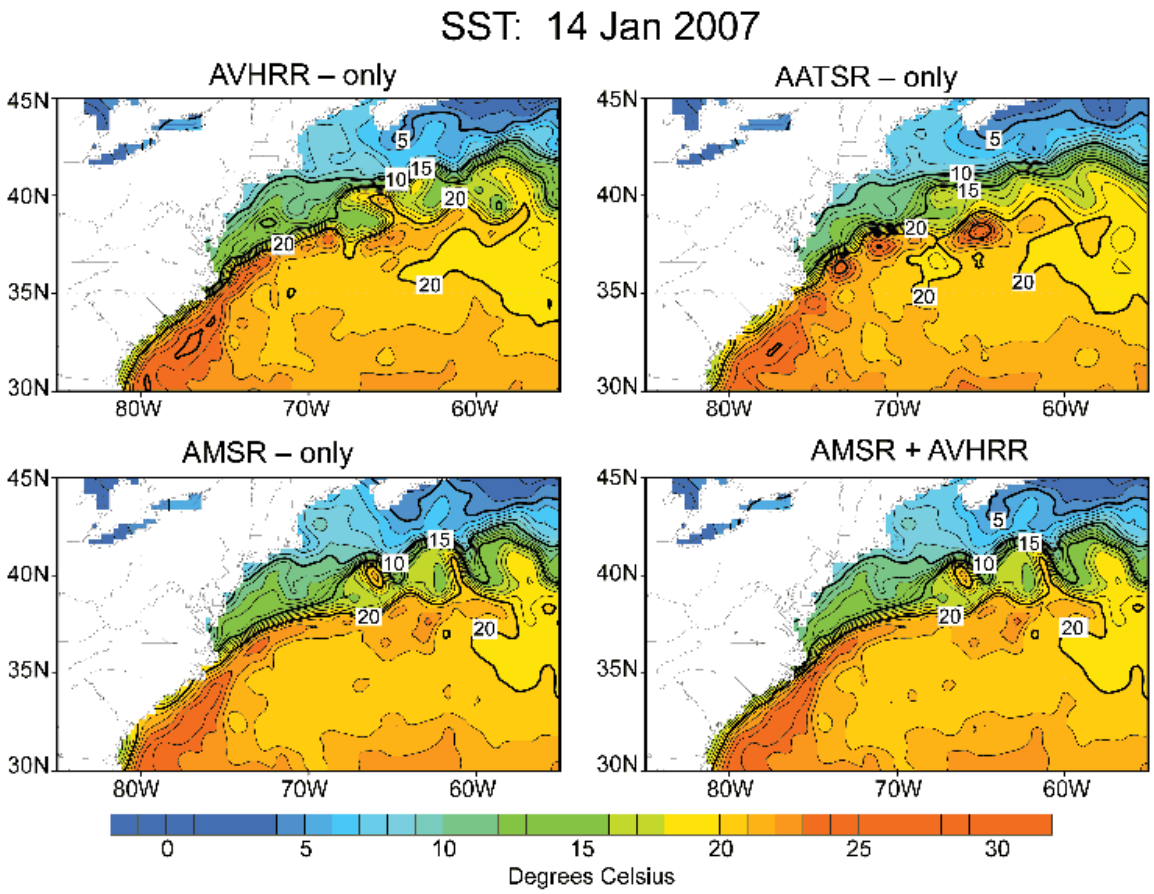

Figure 8. Four daily SST analyses for 14 January 2007. The top left, top right, bottom left and bottom right panels show the daily OI using AVHRR-only, AATSR-only, AMSR-only, and AMSR+AVHRR, respectively.

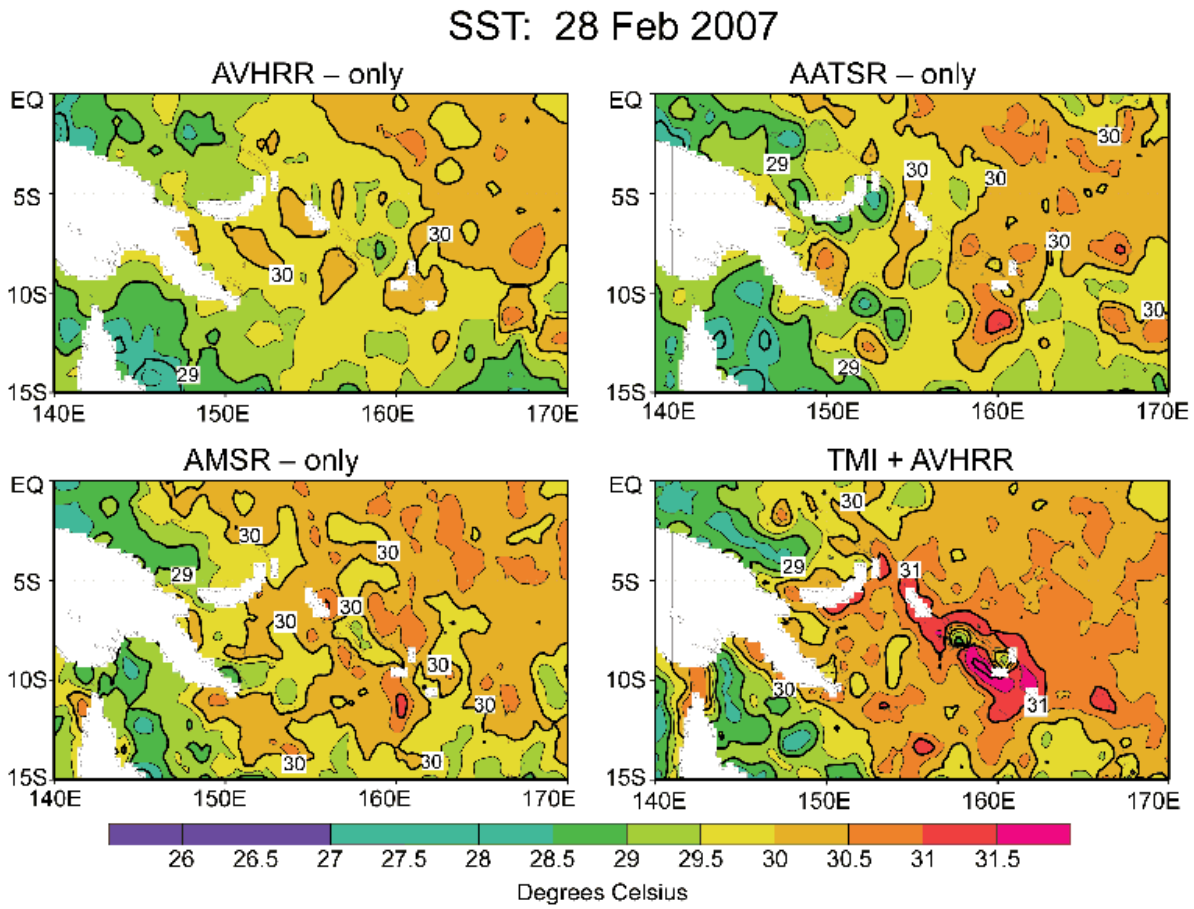

Figure 9. Four daily SST analyses for 28 February 2008. The top left, top right, bottom left and bottom right panels show the daily OI using AVHRR-only, AATSR-only, AMSR-only, and TMI+AVHRR, respectively.

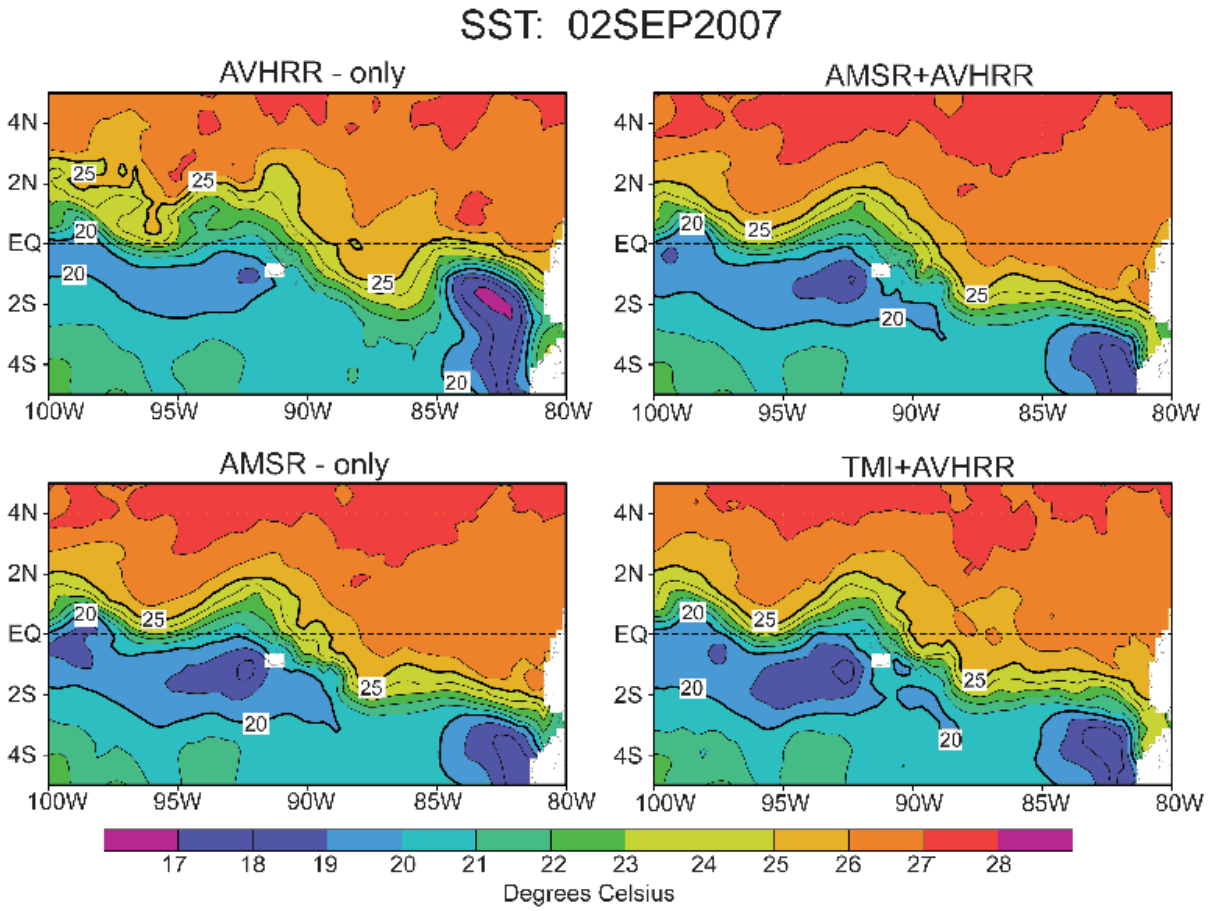

Figure 10. Four daily SST analyses for 28 January 2007. The top left, top right, bottom left and bottom right panels show the daily OI using AVHRR-only, AMSR+AVHRR, AMSR-only, and TMI+AVHRR respectively.

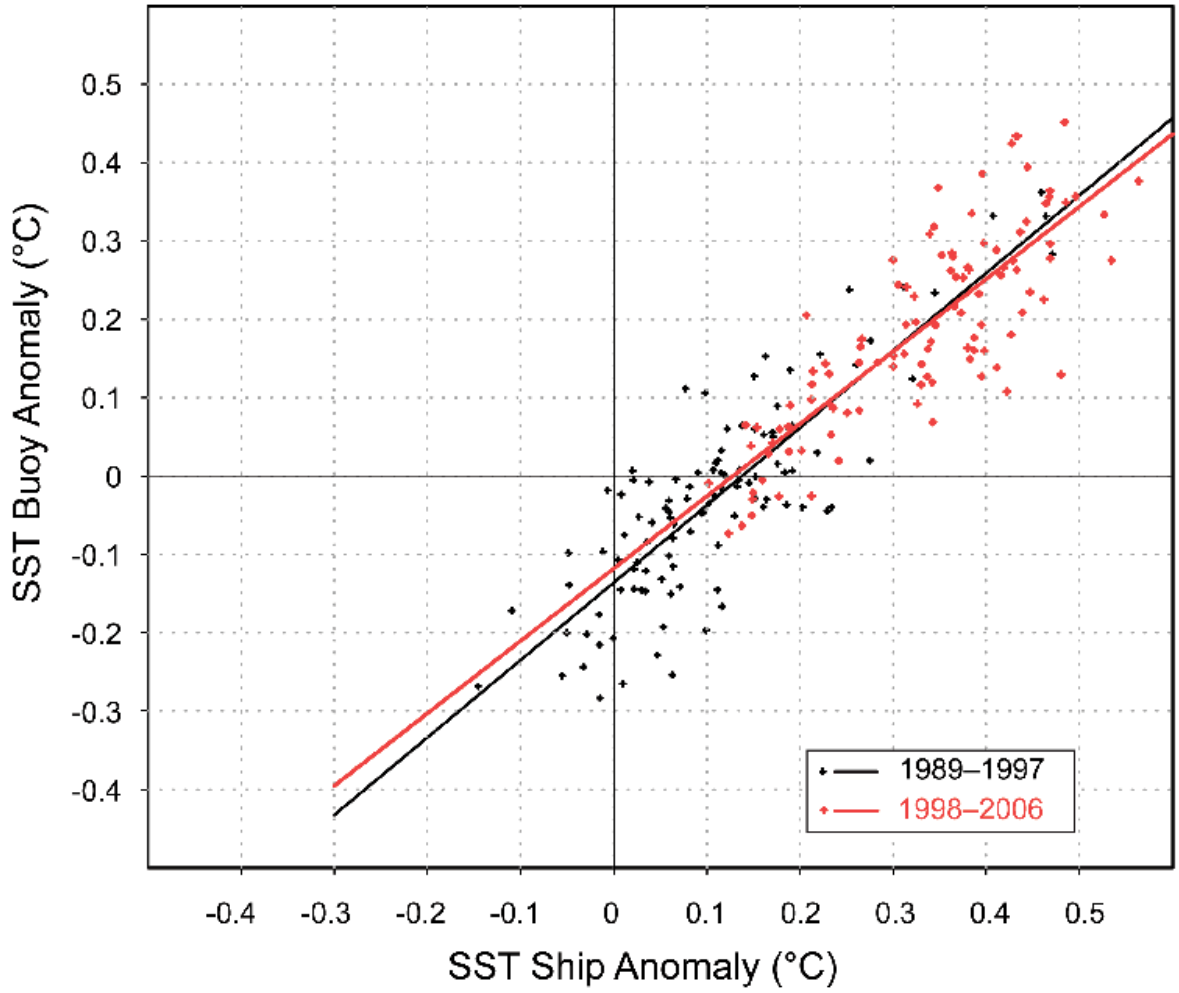

Figure A-1. Scatter plot of global collocated average monthly ship vs. buoy anomaly for January 1989 - December 2006. The first 9-years are shown in the black and the second 9-years in red. Least squares linear fits for the two periods are also shown.